Bridge Pressure Flow Scour

Junke Guo[1], Kornel Kerenyi[2], and Jorge E. Pagan-Ortiz[3]

Abstract: Bridge pressure flow scour is studied analytically and experimentally. The analytical study shows that bridge pressure flow scour depends on the downstream water elevation. For downstream submerged flows, the scour depth is determined by the ratio of inundation to bridge opening, and the shape of bridge deck. The effect of sediment size can be neglected because bridge pressure flows are rapidly varied where the pressure difference dominates the flow processes while the bed shear stress can be neglected. The analytical argument is confirmed by flume experiments with three deck shapes. After considering the effect of deck shape, the pressure flow scour can be described by a cubic equation that can be solved analytically. The relative errors of the predictions by the cubic equation are within 5% the measured scour depths. Finally, a design procedure, with an application example, is presented graphically and analytically.

Keywords: bridge decks, bridge design, bridge foundations, bridge hydraulics, bridge inundation, bridge scour, pressure flows, pressure scour, submerged flows.

Introduction

Bridge is one of the major crossings in road transportation systems. Bridge flows are usually designed to be open channel flow; it nevertheless becomes pressure flow if the bridge is partially or totally submerged during large floods. Unlike open channel flow, pressure flow has a strong scourbility because it can only scour the channel bed to pass a given discharge.

Due to its strong scourbility, pressure flow scour is very important in the design of bridge foundations. This is because poor understanding of pressure flow scour will lead to an inappropriate foundation design, which either significantly increases the cost of a project or results in an unsafe infrastructure. Our current knowledge of the pressure flow scour cannot ensure an efficient design that is safe and economical because most of the previous predictors were derived from free surface flows (Arneson and Abt 1998), which underestimate the scour under pressure flow conditions.

[1]Assistant Professor, Dept. of Civil Engineering, Univ. of Nebraska-Lincoln, PKI 204D, 1110 S 67th ST, Omaha, NE 68182-0178. Email: jguo2@unl.edu

[2]Research Hydraulic Engineer, Office of Infrastructure R&D, Turner-Fairbank Highway Research Center, Federal Highway Administration, 6300 Georgetown Pike, McLean, VA 22101. E-mail: kornel.kerenyi@fhwa.dot.gov

[3]Leader of National Hydraulics Team, Office of Bridge Technology, Federal Highway Administration, 1200 New Jersey Avenue SE, Washington, DC 20590. E-mail: jorge.pagan@fhwa.dot.gov

To better understand pressure flow scour, three systematic studies were reported in literature. Based on the dataset of Colorado State and using a dimensional analysis, Arneson and Abt (1998) proposed the following multiple linear regression equation

$$\frac{y_s}{h_u} = -0.93 + 0.23\left(\frac{h_u}{h_b}\right) + 0.82\left(\frac{y_s + h_b}{h_u}\right) + 0.03\left(\frac{V_b}{V_c}\right) \tag{1}$$

where y_s = scour depth, h_u = depth of the upstream flow, h_b = bridge opening before the scour, V_b = average velocity under the bridge, and V_c = critical velocity of the bed materials

$$V_c = 1.52\sqrt{g\,(s-1)\,d_{50}}\left(\frac{h_u}{d_{50}}\right)^{1/6} \tag{2}$$

where g = gravitational acceleration, s = specific gravity of sediment, and d_{50} = median diameter of the bed materials. Arneson and Abt concluded that the ratio $(y_s + h_b)/h_u$ is the most significant independent, and the ratio V_b/V_c the least. Although Eq. (1) has been adopted in the FHWA manual (Richardson and Davis 2001), it has a serious problem. Just as Lyn (2005) stated, the ratio $(y_s + h_b)/h_u$ is not appropriate to be an independent since y_s/h_u and $(y_s + h_b)/h_u$ in Eq. (1) are almost self-correlated. Lyn further proposed the following power law

$$\frac{y_s}{h_u} = \min\left[0.091\left(\frac{V_b}{V_c}\right)^{2.95}, 0.5\right] \tag{3}$$

where the critical velocity V_c is estimated by Eq. (2). As a result, Lyn believed that the ratio V_b/V_c governs the pressure flow scour.

The third important study of pressure flow scour is by Umbrell et al. (1998) who, using the mass conservation, presented the following equation

$$\frac{y_s + h_b}{h_u} = \frac{V_u}{V_c}\left(1 - \frac{b}{h_u}\right) \tag{4}$$

where V_u = velocity of the approaching flow, and b = thickness of the bridge deck. By comparing Eq. (4) with experimental data, Umbrell et al. modified Eq. (4) as

$$\frac{y_s + h_b}{h_u} = 1.102\left[\frac{V_u}{V_c}\left(1 - \frac{b}{h_u}\right)\right]^{0.603} \tag{5}$$

The problem is when deriving Eq. (4), Umbrell et al. assumed that the under bridge velocity is

the critical velocity V_c. This assumption can only be true if there is no net pressure force; it is not true for bridge transitions because the flow under a bridge is rapidly varied where, like hydraulic jumps, the pressure force dominates the flow processes while the bed shear stress can be neglected. The same reasoning can be applied to Eqs. (1) and (3) for the critical velocity. In brief, our current understanding of the pressure flow scour is far away to its real solution.

The objective of this study is to determine a solution to the pressure flow scour, which can be used to guide practical designs. Specifically, (1) we start with a theoretical analysis that applies the mass and momentum conservation laws to a control volume, which leads to a hypothesis that the major governing independents for pressure flow scour are the deck shape and the ratio of inundation to bridge opening. (2) We then test the hypothesis in a laboratory flume with three deck shapes by varying the bridge opening under the deck, and determine a solution to the pressure flow scour. (3) Finally, we present a procedure to guide practical designs.

Theoretical Analysis

Statement of the Problem

For clarification, the bridge pressure flow scour can be stated as. **Given:** Without contraction channel and piers, a bridge crossing over a river with clear water flow is shown in Fig. 1 where V_u = velocity of the upstream flow, B = width of the river, L = width of the bridge deck, d_{50} = median diameter of the bed materials, h_u = depth of the upstream flow, h_b = bridge opening before the scour, b = thickness of the bridge deck, and L_s = length of the scour hole to the maximum scour depth. **Find:** Determine the maximum scour depth y_s in Fig. 1b by considering a unit river flow.

Analysis: The solution to the problem depends on the downstream water surface elevation. *Case 1:* If the downstream low chord of the bridge is unsubmerged, shown in Fig. 1b, the bridge operates as a sluice gate. In such a case, the bridge flow is partially pressurized, and the gravity or Froude number affects the scour depth. *Case 2:* If the bridge downstream is partially submerged, shown in Fig. 2a, the bridge operates as an orifice so that the net pressure force on the control surfaces dominates the scour depth; and the effect of Froude number can be neglected. *Case 3:* If the bridge is totally submerged into water, the bridge operates as the combination of an orifice and a weir; only the discharge under the bridge affects the scour depth.

The scour depth in Case 1 is less than those in Cases 2 and 3. This is because in Case 1, the flow can adjust its depth through both the free surface and erosive bed, whereas in Case 2 or 3 the

flow can only adjust its depth by scouring the channel bed. Therefore, Case 1 is trivial in practice, and in the following we discuss only Cases 2 and 3.

Solution to Case 2

Consider the control volume in Fig. 2b, where q_0 is the unit discharge of the river, q_1 is the unit discharge under the bridge, V_b is the cross-sectional velocity at the maximum scour, a is the depth of bridge inundation, $\mathcal{D}$ is the drag of bridge deck, $\mathcal{R}$ is the frictional force or resultant force of the bed shear stress in the flow direction, and $\mathcal{P}$ is the resultant force of pressure on the control surfaces in the flow direction. The rest of the symbols are the same as those in Fig. 1.

Applying the conservation of mass to the control volume in Fig. 2b gives

$$q_0 = q_1 \tag{6}$$

where

$$q_0 = V_u h_u \tag{7}$$

Applying the conservation of momentum gives

$$\mathcal{P} - \mathcal{R} - \mathcal{D} = (\rho V_u)(-q_0) + (\rho V_b)(q_1) \tag{8}$$

where ρ = density of water, the momentum coefficients are assumed to be 1. Substituting Eq. (6) into Eq. (8) yields

$$\mathcal{P} - \mathcal{R} - \mathcal{D} = \rho q_1 (V_b - V_u) \tag{9}$$

The frictional force $\mathcal{R}$, pressure force $\mathcal{P}$, and drag $\mathcal{D}$ are detailed as follows.

Frictional force $\mathcal{R}$: When the scour hole reaches its equilibrium state, the shear stress on the bed is a critical shear stress τ_c everywhere. Referring to Fig. 2c, consider a differential length dl along the curved bed, the differential shear force is then $\tau_c dl$, and its component in the negative flow direction is $\tau_c dl \cos\theta = \tau_c dx$ where θ = angle between the local bed surface and the flow direction. Therefore, the frictional force is

$$R = \int_0^{L_s} \tau_c dx = \tau_c L_s \tag{10}$$

where L_s = length of the scour hole to the maximum scour depth, shown in Fig. 1b, and the critical

shear stress τ_c can be obtained from the Shields diagram for a given sediment size.

Pressure force $\mathcal{P}$: The pressure on the control surfaces include two parts: hydrostatic and hydrodynamic. The net hydrostatic force on the control surfaces in the flow direction is zero. Thus, the pressure force $\mathcal{P}$ results from the net hydrodynamic force, which can be written as

$$\mathcal{P} = \mathcal{P}\left(\rho, V_u, a, y_s\right) \tag{11}$$

The deck inundation a and the scour depth y_s are involved since both alternate the original streamlines and affect the hydrodynamic pressure. According to the Buckingham Π theorem, if choosing ρ, V_u and a as repeating variables, we can rearrange Eq. (11) in dimensionless form

$$\frac{\mathcal{P}}{\frac{1}{2}\rho V_u^2 a} = C_{\mathcal{P}}\left(\frac{y_s}{a}\right) \tag{12}$$

where $C_{\mathcal{P}}$, defined as a pressure coefficient, varies with y_s/a, and the constant $1/2$ is just for convenience of analysis. Eq. (12) gives

$$\mathcal{P} = C_{\mathcal{P}}\left(\frac{y_s}{a}\right) \cdot \frac{1}{2}\rho V_u^2 a \tag{13}$$

Drag $\mathcal{D}$: The drag $\mathcal{D}$ due to the bridge deck can be written as

$$\mathcal{D} = \frac{C_{\mathcal{D}}}{2}\rho V_u^2 a \tag{14}$$

where $C_{\mathcal{D}}$ = drag coefficient of the deck, which varies with the shape of deck.

Substituting Eqs. (10), (13) and (14) into Eq. (9) gives

$$\left[C_{\mathcal{P}}\left(\frac{y_s}{a}\right) - C_{\mathcal{D}}\right] \cdot \frac{1}{2}\rho V_u^2 a - \tau_c L_s = \rho q_1 \left(V_b - V_u\right) \tag{15}$$

Diving both sides of the above equation by $\rho V_u^2 a/2$ results in the dimensionless equation

$$C_{\mathcal{P}}\left(\frac{y_s}{a}\right) - C_{\mathcal{D}} - \frac{2\tau_c L_s}{\rho V_u^2 a} = \frac{2q_1}{aV_u}\left(\frac{V_b}{V_u} - 1\right) \tag{16}$$

which can be further simplified by applying Eqs. (6) and (7). Considering

$$q_1 = q_0 = V_u h_u = V_u\left(h_b + a\right) \tag{17}$$

where the geometric relation $h_u = h_b + a$ is from Fig. 2a, and

$$V_b = \frac{q_1}{h_b + y_s} = \frac{h_b + a}{h_b + y_s} V_u \tag{18}$$

the right-hand-side of Eq. (16) becomes

$$\frac{2q_1}{aV_u}\left(\frac{V_b}{V_u} - 1\right) = 2\left(\frac{h_b + a}{h_b + y_s}\right)\left(\frac{a - y_s}{a}\right) \tag{19}$$

Replacing the right-hand-side of Eq. (16) with Eq. (19) gives

$$\overbrace{\underbrace{C_{\mathcal{P}}\left(\frac{y_s}{a}\right) - C_{\mathcal{D}}}_{\text{pressure + drag}} - \underbrace{\frac{2\tau_c L_s}{\rho V_u^2 a}}_{\text{friction}}}^{\text{dimensionless total force}} = \underbrace{2\left(\frac{h_b + a}{h_b + y_s}\right)\left(\frac{a - y_s}{a}\right)}_{\text{denoted as } Z \text{ in Table 1}} \tag{20}$$

Unfortunately, both $C_{\mathcal{P}}$ and $C_{\mathcal{D}}$ are unknown in this study. To avoid many empirical equations, we skip the interim expression of $C_{\mathcal{P}}\left(y_s/a\right)$ and directly find a solution for the scour depth y_s. Multiplying through Eq. (20) by $a/(a - y_s)$ gives

$$\left(\frac{a}{a - y_s}\right)\left[C_{\mathcal{P}}\left(\frac{y_s}{a}\right) - C_{\mathcal{D}} - \frac{2\tau_c L_s}{\rho V_u^2 a}\right] = 2\left(\frac{h_b + a}{h_b + y_s}\right) \tag{21}$$

Taking the reciprocal of the above gives

$$\left(\frac{a - y_s}{a}\right)\left[C_{\mathcal{P}}\left(\frac{y_s}{a}\right) - C_{\mathcal{D}} - \frac{2\tau_c L_s}{\rho V_u^2 a}\right]^{-1} = \frac{1}{2}\frac{h_b + y_s}{h_b + a} \tag{22}$$

Since

$$\frac{h_b + y_s}{h_b + a} = 1 - \frac{a - y_s}{h_b + a} \tag{23}$$

Eq. (22) can be rewritten as

$$\left(\frac{a - y_s}{a}\right)\left[C_{\mathcal{P}}\left(\frac{y_s}{a}\right) - C_{\mathcal{D}} - \frac{2\tau_c L_s}{\rho V_u^2 a}\right]^{-1} = \frac{1}{2} - \frac{1}{2}\frac{a - y_s}{h_b + a} \tag{24}$$

Rearranging it gives

$$\frac{a - y_s}{h_b + a} = 1 - 2\left(\frac{a - y_s}{a}\right)\left[C_{\mathcal{P}}\left(\frac{y_s}{a}\right) - C_{\mathcal{D}} - \frac{2\tau_c L_s}{\rho V_u^2 a}\right]^{-1} \tag{25}$$

Multiplying through the above equation by $a/\left(a-y_s\right)$ gives

$$\frac{a}{h_b+a}=\frac{a}{a-y_s}-2\left[C_{\mathcal{P}}\left(\frac{y_s}{a}\right)-C_{\mathcal{D}}-\frac{2\tau_c L_s}{\rho V_u^2 a}\right]^{-1} \tag{26}$$

which is equivalent to

$$\frac{a}{h_b+a}=F\left(\frac{y_s}{a},C_{\mathcal{D}},\frac{\tau_c L_s}{\rho V_u^2 a}\right) \tag{27}$$

where the function F will be determined experimentally. Eq. (27) leads to a hypothesis: the dimensionless pressure flow scour, y_s/a, depends on the ratio of inundation to bridge opening, a/h_b, the deck drag coefficient, $C_{\mathcal{D}}$, and the dimensionless critical shear stress $\tau_c L_s/\rho V_u^2 a$. We will test this hypothesis and determine the function F, after discussing the solution to Case 3.

Solution to Case 3

The governing equation (9) for Case 2 is also valid for Case 3 if considering $q_1=q_0-q_2$ in Fig. 3b. This claim can be proved by applying the laws of mass and momentum conservation to the control volume in Fig. 3b. Following Umbrell et al. (1998), the overflow velocity is assumed the same as the upstream velocity V_u, which gives the unit overflow discharge q_2 as

$$q_2=V_u\left(h_u-h_b-b\right) \tag{28}$$

This assumption is just a rough approximation, the error due to this assumption will be corrected using empirical model constants later. The mass conservation gives

$$q_0=q_1+q_2 \tag{29}$$

and the momentum conservation leads to

$$\mathcal{P}-\mathcal{R}-\mathcal{D}=\left(\rho V_u\right)\left(-q_0\right)+\left(\rho V_u\right)\left(q_2\right)+\left(\rho V_b\right)\left(q_1\right) \tag{30}$$

Substituting Eq. (29) into Eq. (30) results in

$$\mathcal{P}-\mathcal{R}-\mathcal{D}=\rho q_1\left(V_b-V_u\right) \tag{31}$$

which is the same as Eq. (9). Thus, Eq. (27) is also applicable for Eq. (31) except that the inundation a is replaced with the deck thickness b, i.e., $a = b$ in Case 3.

In brief, Case 1 is trivial in terms of design because the scour depth is not as deep as those in Cases 2 and 3; Cases 2 and 3 are described with Eq. (9) or (31). The scour depth y_s can be obtained by studying the function F in Eq. (27) experimentally.

Experimental Approach

The objective of this section is to test the hypothesis that the relative pressure flow scour is determined by the deck drag coefficient and the ratio of inundation to bridge opening, and to find an expression of Eq. (27). To this end, we conducted a series of flume experiments in the FHWA Hydraulics Laboratory, located at the Turner-Fairbank Highway Research Center in McLean, VA. The experimental set-up and data analysis are described as follows.

Experimental set-up

Flume system: Fig. 4a shows an overview of the experimental flume; and Fig. 4b details the flume system. The flume is rectangular, 21.35 m long and 1.83 m wide with glass sides and stainless steel bottom. As shown in Fig. 4b, in the middle of the flume was installed a test section 0.63 m wide and 2.8 m long, together with a model bridge deck. A honeycomb flow straightener and a trumpet-shaped inlet were carefully designed to smoothly guide the flow into the test channel. Referring to the side view in Fig. 4b, a 40-cm sediment recess, which is amplified in Fig. 5, on the flume bottom and under the bridge was installed for local scour information. The flume was set horizontally, and an adjustable tailgate located at the downstream end of the flume controlled the depth of flow. A circulation system with a sump and a pump supplied water in the flume. The capacity of the sump was 210 m^3 while the pump output rate could vary between 0 and 0.3 m^3/s. In addition, an electromagnetic flow meter measured the discharge.

Sand bed preparation: Fig. 5 shows the sand bed preparation in the test channel. The median bed material diameter was $d_{50} = 1$ mm; a 20-cm thick layer of sand was distributed evenly on the flume bottom. The sediment recess on the flume bottom could model a local scour depth til 60 cm. According to the Shields diagram, the critical shear stress for $d_{50} = 1\,\text{mm}$ is about $\tau_c = 0.05\,\text{Pa}$.

Model decks: Three model decks, made of special Plexiglas and shown in Fig. 6, were used in the experiments. Fig. 6a shows a 3D view of the 6-girder deck, while Fig. 6b-d show the cross-sections of

the three model decks. The 6-girder deck was chosen since most bridges with 4-lanes have 6-girders, while the 3-girder deck corresponds to bridges with 2-lanes. For comparison, a streamline deck was also tested since it has the least scour depth. The deck elevation was adjustable, permitting the deck to have 8 bridge openings.

Determination of the operating discharge: This study emphasizes clear water scour since it is usually larger than the corresponding live bed scour. To ensure a clear water scour under the bridge, the approach velocity in the test channel must be less than the critical velocity, which can be estimated by Eq. (2). Since the flow depths in the experiments were always kept 25 cm, according to Eq. (2), the critical velocity is about

$$V_c = 0.485 \text{ m/s}$$

which corresponds to a maximum allowable discharge in the test channel

$$Q_{\max} = (0.485\,\text{m/s})\,(0.63\,\text{m})\,(0.25\,\text{m}) = 0.0764 \text{ m}^3/\text{s} = 76.4 \text{ l/s}$$

where 0.63 m is the width of the test section. The operating discharge was then chosen as 64.6 l/ s, which corresponds to an approach velocity $V_u = 0.41\,\text{m/s}$ in the test channel, Reynolds number $\text{Re} = 2.3 \times 10^5$, and Froude number $\text{Fr} = 0.35$.

Data collection: An automated flume carriage fitted to the main flume, shown in Fig. 7, was used to collect data of velocity field and scour depths. The scour depths were measured using a laser distance sensor while the velocity field using a PIV system. A LabVIEW programming was applied for data acquisition, instrument control, data analysis, and report generation. Fig. 8 illustrates a scour profile and a velocity field around the bridge.

Experimental procedures: 1) Made the sediment bed in the test section like that in Fig. 5; 2) installed a bridge deck and positioned it perpendicular to the direction of flow; 3) adjusted the elevation of the deck to a designed bridge opening; 4) pumped water from the sump to the flume gradually from 0 to 64.6 l/ s, which could be checked with the electromagnetic flow meter; 5) run each experiment for 48 hours so that the scour hole could reach its equilibrium state; and 6) mapped the scour hole using the laser distance sensor.

For each deck, experiments with 8 bridge openings were tested. For each opening, the test was repeated; and the average of the two maximum scour depths was used for the data analysis.

Data analysis and interpretation

Fig. 8a shows the maximum scour depth is near the downstream edge of the deck. Similar patterns were found under the 3-girder deck and the streamline deck. Thus, we can approximate the distance from the bridge entrance to the maximum scour depth is

$$L_s \approx L = 0.26\,\mathrm{m} \tag{32}$$

Table 1 lists the experimental results for the three deck shapes. In columns 1 to 3 are the bridge opening h_b, inundation a, and measured scour depth y_s, respectively. Column 4 shows the value of dimensionless scour depth y_s/a. In the following analysis, we concentrate only on Cases 2 and 3, as marked in column 11 in Table 1.

Test of the effect of friction on the scour depth: Like a hydraulic jump, bridge pressure flows are rapidly varied. In such a flow, the effect of friction may be neglected. This hypothesis can be tested quantitatively. The dimensionless total force can be estimated by calculating the right-hand-side of Eq. (16) or (19), which is listed in column 5 in Table 1; the dimensionless frictional force can be estimated by the friction term in Eq. (20), tabulated in column 6; and the ratio of friction to total force is in column 7. We plot column 7 versus column 4 in Fig. 9 where the negative sign in the ordinate means the total force points upstream. Fig. 9 shows that the contribution of friction to the total force is less that 8% for all the measurements, which confirms our hypothesis that the frictional force can be neglected. Thus, Eq. (20) becomes

$$C_{\mathcal{P}}\left(\frac{y_s}{a}\right) - C_{\mathcal{D}} = 2\left(\frac{h_b + a}{h_b + y_s}\right)\left(\frac{a - y_s}{a}\right) \tag{33}$$

Furthermore, Eq. (27) reduces to

$$\frac{a}{h_b + a} = F\left(\frac{y_s}{a}, C_{\mathcal{D}}\right) \tag{34}$$

Test of the effect of drag coefficient on the scour depth: The effect of drag coefficient can be tested by plotting Eq. (33). Our measurements showed that the drag coefficient C_D is about 1 for the streamline deck, 2 for the 3-girders deck, and 2.5 for the 6-girders. The drag study will be reported separately. To test the effect of drag coefficient, we can make a working hypothesis like this: If the drag coefficient C_D has a significant effect on the scour depth, a plot of the right-hand-side of Eq. (33) versus y_s/a will yield three different curves; otherwise, the effect of drag coefficient can be neglected. The values of column 5 versus column 4 are plotted in Fig. 10, which clearly

shows that all the data from the three deck shapes collapse into a single curve. This means the effect of drag coefficient can be neglected. Therefore, Eq. (34) further reduces to

$$\frac{a}{h_b + a} = F\left(\frac{y_s}{a}\right) \tag{35}$$

Test of the effect of inundation on the scour hole: This test is straightforward. We simply plot Eq. (35), according to columns 4 and 8, in Fig. 11 that shows a clear correlation between $a/(h_b + a)$ and y_s/a. We can see that the data of the streamline and the 6-girders decks form a smoothly connected curve, which can be approximated as

$$\frac{a}{h_b + a} = 0.1628Y^3 - 0.3203Y^2 + 0.3949Y \tag{36}$$

However, the data for the 3-girders deck is slightly above those for the 6-girders deck. We will collect more data to see wether it is a systematic error or a slight effect of drag coefficient.

To sum up, the bridge pressure flow scour mainly depends on the ratio of inundation to bridge opening; the effects of the drag coefficient and the sediment size or friction can be neglected.

Design Procedures and Application Example

The design procedures are very simple by applying the proposed equation (36). Given a design discharge q per unit width, bridge opening h_b, and deck thickness b, the scour depth y_s can be estimated by the following steps:

Step 1: Use HEC-RAS for gradually varied flows or the Manning equation for uniform flows to estimate the upstream flow depth h_u.

Step 2: Calculate the inundation depth a by

$$a = \min\{h_u - h_b, b\} \tag{37}$$

where $a = h_u - h_b$ for Case 2 without overflow, $a = b$ for Case 3 with overflow.

Step 3: Calculate the value of $a/(h_b + a)$, and read the value of $Y = y_s/a$ from Fig. 11 or solve for Y in Eq. (36), which has two imaginary solutions and one positive solution. The scour depth is

embedded in the positive solution that can be analytically found by

$$Y = \left(\sqrt{0.054096 + r^2} + r\right)^{1/3} - \left(\sqrt{0.054096 + r^2} - r\right)^{1/3} + 0.656\,02 \tag{38}$$

where

$$r = \frac{3.0717a}{h_b + a} - 0.51332 \tag{39}$$

The derivations of the above two equations are detailed in Appendix. To check the accuracy of Eq. (38), the calculated scour depth for each measurement is tabulated in Table 1 in column 9, and the corresponding relative error in column 10. We can see that except for Case 1, all the calculated scour depths are within 5% the measured values.

Example This example is from HEC-18 (Richardson and Davis 2001, p6.32). An existing bridge is subjected to pressure flow to the top of a solid guard rail at the 100-year return period flow. There is only a small increase in flow depth at the bridge for the 500-year return period due to the large overbank area. The bed materials are $d_{50} = 0.4\,\text{mm}$. The bridge opening is $h_b = 7.93\,\text{m}$ before scour. Calculate the vertical contraction scour.

Step 1: According to HEC-18, a HEC-RAS model with 500-year flood gives

$$h_u = 9.75\,\text{m}, \quad V_u = 2.93\,\text{m/s}, \quad q_1 = 28.56\,\text{m}^2/\text{s} \tag{40}$$

Step 2: According to the problem statement, there is only a small increase in flow depth so that we assume the bridge is only partially inundated, without overflow. The inundation depth is then

$$a = h_u - h_b = 9.75 - 7.93 = 1.82\,\text{m} \tag{41}$$

Step 3: Calculate the value

$$\frac{a}{h_b + a} = \frac{a}{h_u} = \frac{1.82}{9.75} = 0.186\,67 \tag{42}$$

which gives

$$r = \frac{3.0717a}{h_b + a} - 0.51332 = (3.0717)\,(0.18667) - 0.51332 = 0.06 \tag{43}$$

$$
\begin{aligned}
Y &= \left(\sqrt{0.054096+r^2}+r\right)^{1/3}-\left(\sqrt{0.054096+r^2}-r\right)^{1/3}+0.656\,02 \\
&= \left(\sqrt{0.054096+(0.06)^2}+0.06\right)^{1/3}-\left(\sqrt{0.054096+(0.06)^2}-0.06\right)^{1/3}+0.656\,02 \\
&= 0.760\,77
\end{aligned}
$$

The scour depth is then

$$y_s = (0.76)\,(1.82) = 1.383\,\mathrm{m} \tag{44}$$

For comparison, HEC-18 gives $y_s \approx 11\,\mathrm{m}$, which might be too deep.

Note that flow velocity or design discharge is implicitly embedded in the determination of the flow depth h_u, in Step 1, through the Manning equation for upstream uniform flows, or a HEC-RAS procedure for gradually varied flows. For different discharges, we have different upstream depth h_u and different inundation a. Furthermore, we have different scour depth y_s. Therefore, the scour depth y_s implicitly depends on flow conditions.

Conclusions

The following conclusions can be drawn from this study.

1. Bridge pressure flow scour can be divided into three cases according to the downstream water surface elevations. Case 1 where the bridge operates as a sluice gate, is trivial in terms of design. Cases 2 and 3 where the bridge operates as an orifice, can be described by a momentum equation.

2. The theoretical analysis shows that relative bridge pressure flow scour is determined by the ratio of the inundation to bridge opening, and the drag coefficient, and the dimensionless critical shear stress, as described by Eq. (27).

3. The experiments show that: i) the friction contribution to the total force is less than 8%, shown in Fig. 9. The effect of friction on the scour depth can then be neglected; ii) the effect of the drag coefficient can also be neglected. (This will be further confirmed.); and iii) the pressure flow scour mainly depends on the ratio of inundation to bridge opening, and increases with the ratio of the inundation to bridge opening, as shown in Fig. 11.

4. The bridge pressure flow scour can be predicted by the empirical equation (36), which has been validated with the data of three decks, shown in Fig. 11, within 5% the measured values.

5. The design of scour depth can be estimated graphically in Fig. 11, or analytically by Eq. (38) with Eq. (39). The proposed procedure needs a design discharge, the bridge opening, and deck thickness. Note that the prerequisites of application are: i) the river bed is erodible although the critical shear stress is neglected; and ii) the scour hole has reached its equilibrium state.

Acknowledgement

This research was supported by the Federal Highway Administration's Hydraulics R&D Program with Contract No. DTFH61-04-C-00037.

Appendix: Solution of the Scour Depth Equation

Rearranging Eq. (27) as

$$AY^3 + BY^2 + CY + D = 0 \tag{A-1}$$

where $A = 0.1628$, $B = -0.3204$, $C = 0.3949$, and $D = -a/(h_b + a)$. According to a root-finding formula at http://en.wikipedia.org/wiki/Cubic_equation, the real root of the above equation can be found by the following:

$$q = \frac{3AC - B^2}{9A^2} = \frac{3\,(0.1628)\,(0.3949) - (-0.3204)^2}{9\,(0.1628)^2} = 0.378\,20 \tag{A-2}$$

$$\begin{aligned} r &= \frac{9ABC - 27A^2D - 2B^3}{54A^3} \\ &= \frac{9\,(0.1628)\,(-0.3204)\,(0.3949) - 27\,(0.1628)^2\,D - 2\,(-0.3204)^3}{54\,(0.1628)^3} \\ &= -3.071\,3D - 0.513\,32 \end{aligned} \tag{A-3}$$

$$\begin{aligned} Y &= \left(\sqrt{q^3 + r^2} + r\right)^{1/3} - \left(\sqrt{q^3 + r^2} - r\right)^{1/3} - \frac{B}{3A} \\ &= \left(\sqrt{(0.378\,20)^3 + r^2} + r\right)^{1/3} - \left(\sqrt{(0.378\,20)^3 + r^2} - r\right)^{1/3} + \frac{0.3204}{3\,(0.1628)} \\ &= \left(\sqrt{0.054096 + r^2} + r\right)^{1/3} - \left(\sqrt{0.054096 + r^2} - r\right)^{1/3} + 0.656\,02 \end{aligned} \tag{A-4}$$

where r is determined by Eq. (A-3).

Notation

The following symbols are used in this paper:

A, B, C, D = parameters in Eq. (A-1)
a = depth of bridge inundation
b = thickness of bridge deck
$C_{\mathcal{D}}$, $C_{\mathcal{P}}$ = drag and pressure coefficient, respectively
$\mathcal{D}$ = drag of bridge deck
d_{50} = median diameter of sediment
F = functional symbol
Fr = Froude number
g = gravitational acceleration
h_b = bridge opening
h_u = flow depth approaching to bridge
L = width of bridge, shown in Fig. 1a
L_s = length of scour hole to the maximum scour depth
l = length along a curved bed
$\mathcal{P}$ = net pressure force
$Q_{\max}$ = maximum allowable discharge in the flume
q = parameter in Eq. (A-2)
q_0 = unit discharge approaching to the bridge
q_1 = unit discharge under the bridge
q_2 = unit discharge over the bridge
$\mathcal{R}$ = frictional force on the channel bed
Re = Reynolds number
r = parameter in Eqs. (39) and (A-3)
s = specific gravity of sediment
SH = shape constant
V_c = critical velocity
V_b = velocity under the bridge at the maximum scour depth
V_u = velocity approaching the bridge
Y = dimensionless scour depth, $Y = y_s/a+\mathrm{SH}$
y_s = maximum scour depth
ρ = density of water
τ_c = critical shear stress

References

Arneson, L. A., and Abt, S. R. (1998). "Vertical contraction scour at bridges with water flowing under pressure conditions." *Transportation Research Record.* 1647, 10-17.

Lyn, D. A. (2005). "Pressure-flow scour: a re-examination of the HEC-18 equation." Proc. ASCE World Environmental and Water Resources Congress 2006, Omaha, NE.

Richardson, E. V., and Davis, S. R. (2001). *Evaluating scour at bridges.* HEC-18, FHWA-NH-01-001, 4th Ed., U.S. Dept. of Transp., Washing, D.C.

Umbrell, E. R., Young, G. K., Stein, S. M., and Jones, J. S. (1998). "Clear-water contraction scour under bridges in pressure flow." *J. Hydraul. Engrg.*, 124(2), 236-240.

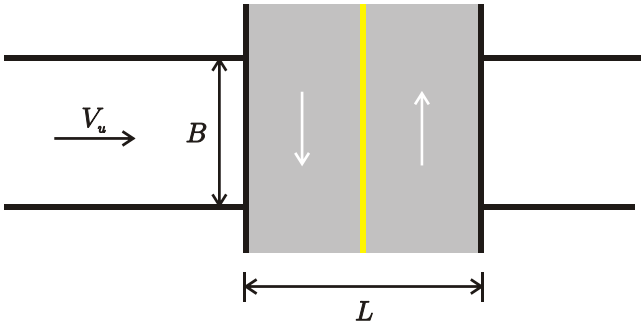

(a) Plan of a bridge crossing

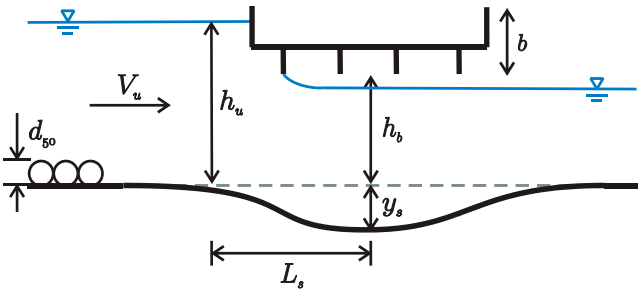

(b) Centerline cross-section

Fig. 1: Flow through bridge without contraction channel and piers

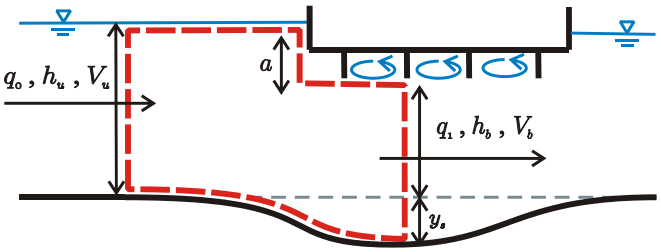

(a) River centerline cross-section

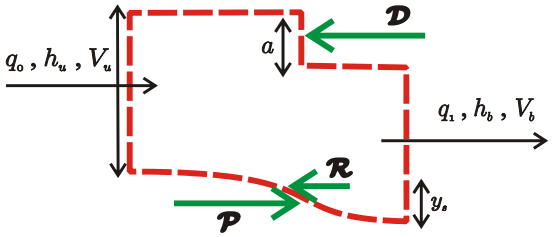

(b) Control volume analysis

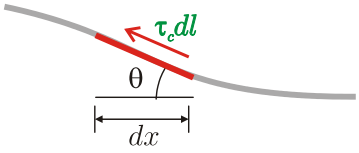

(c) Analysis of frictional force

Fig. 2: Bridge operating as an orifice

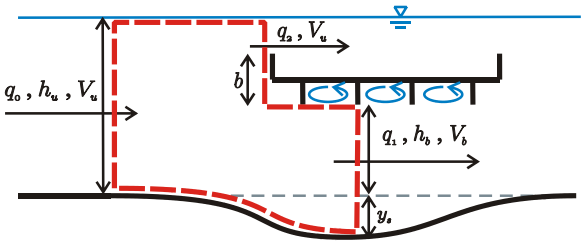

(a) River centerline cross-section

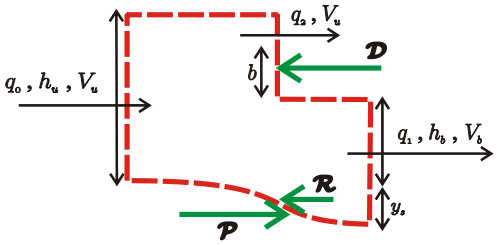

(b) Control volume analysis

Fig. 3: Bridge operationg as the combination of an orifice and a weir

(a) Overview of the flume

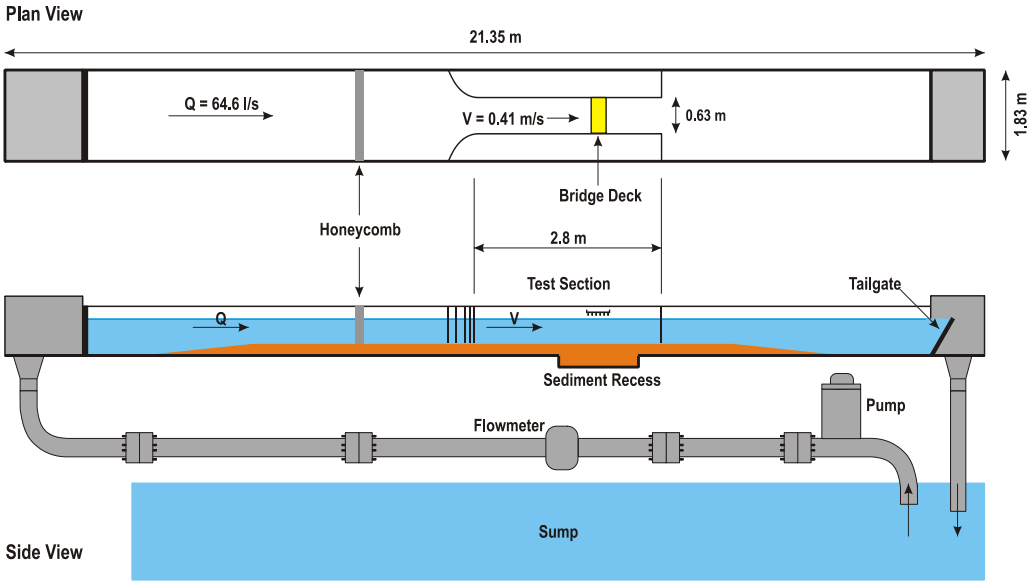

(b) The flume system

Fig. 4: Experimental apparatus

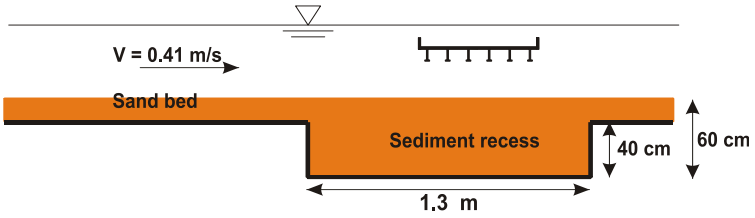

Fig. 5: Sand bed preparation in the test section

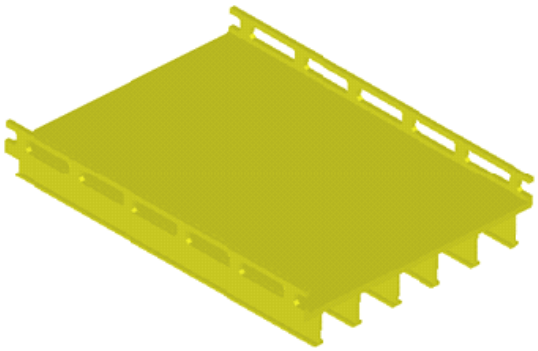

(a) 3D view of the 6-girder deck

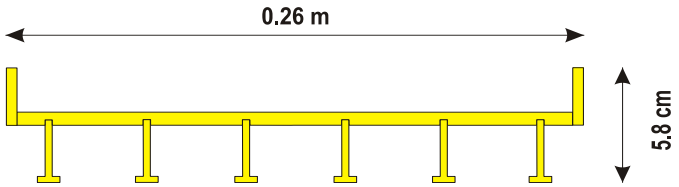

(b) Cross-section of the 6-girder deck

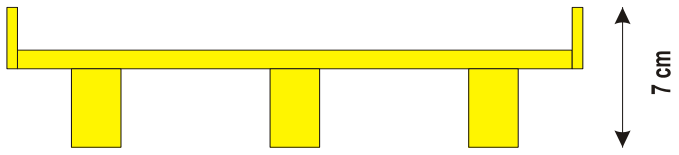

(c) Cross-section of the 3-girder deck

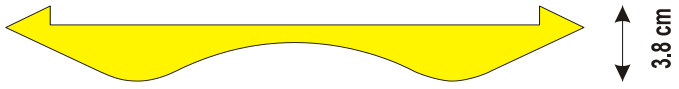

(d) Cross-section of the streamline deck

Fig. 6: Model decks of the experiments

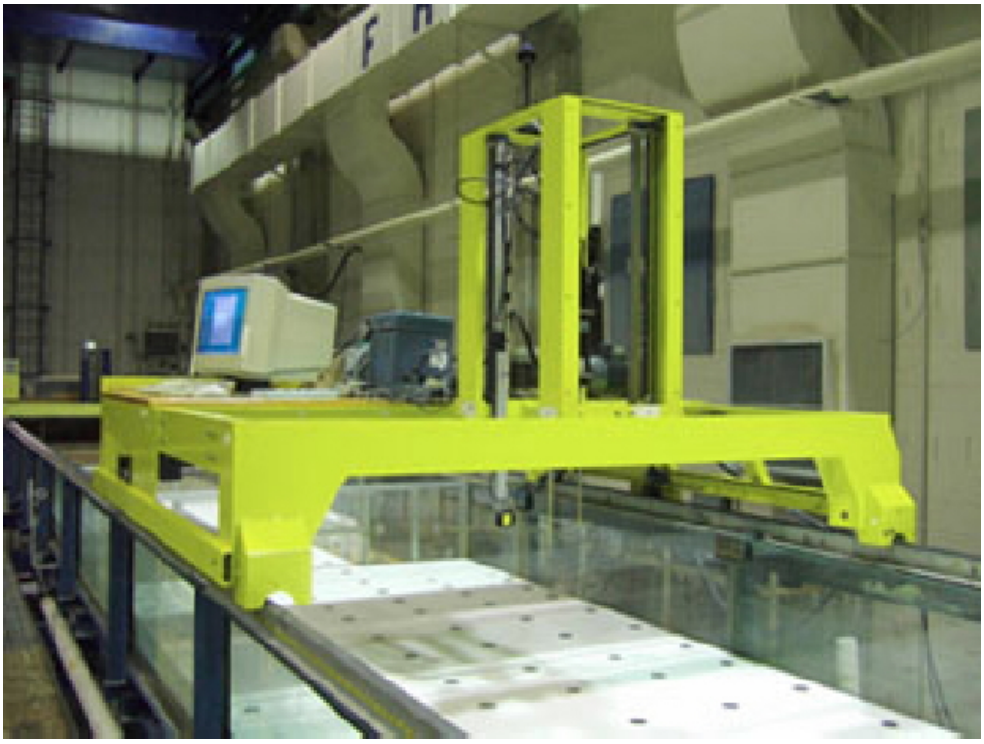

Fig. 7: The automated flume carriage fitted to the main flume.

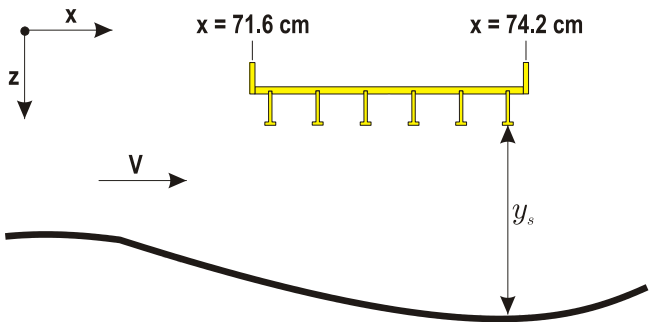

(a) Profile of a scour hole measured using the laser distance sensor

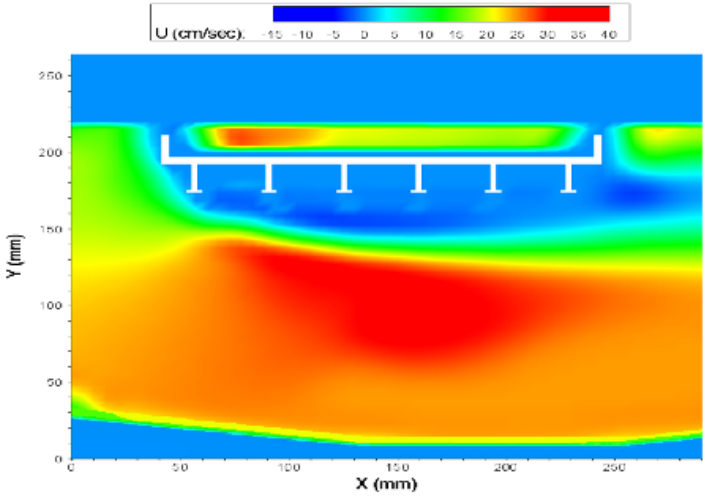

(b) Velocity field around the bridge measured using the PIV system

Fig. 8: Samples of measurements

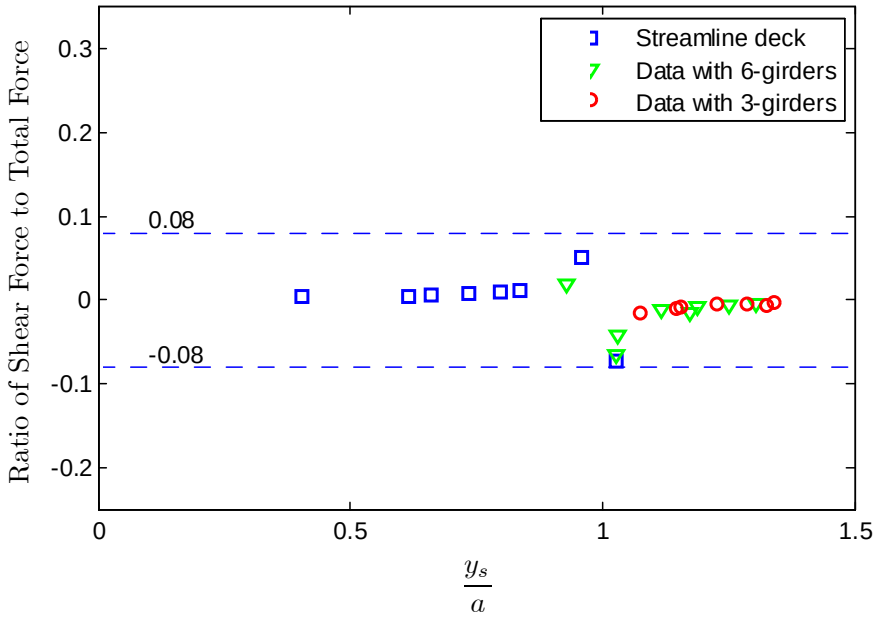

Fig. 9: Test of the effect of friction on the total force

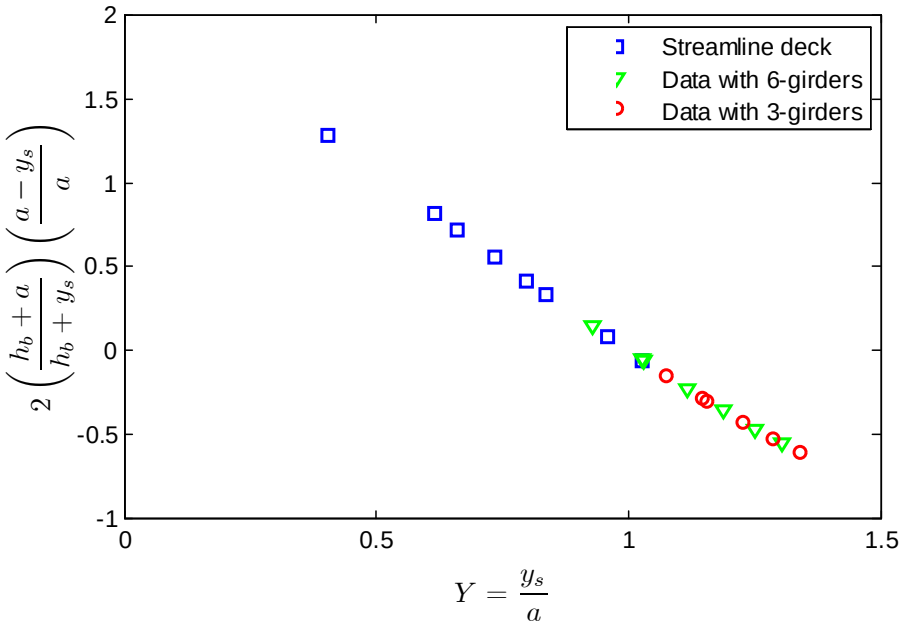

Fig. 10: Test of the effect of drag coefficient on scour depth

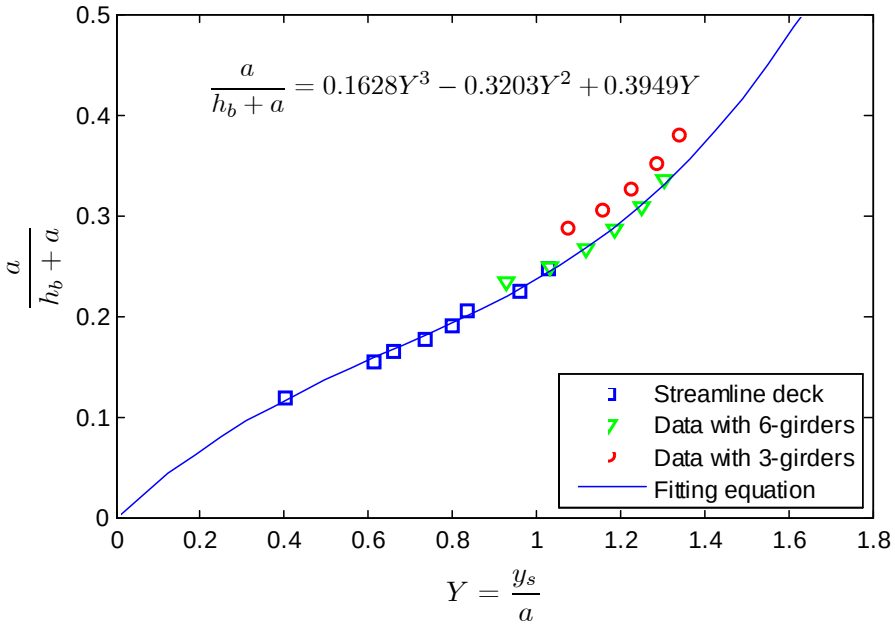

Fig. 11: Test of the effect of inundation on the scour depth

Table 1: Summary of experimental results

h_b cm	a cm	Measured y_s, cm	$\frac{y_s}{a}$	Dimensionless Total Force	$\frac{2\tau_c L_s}{\rho V_u^2 a}$	Friction / Total Force	$\frac{a}{h_b + a}$	Calculated y_s, cm	Error %	Remark
(1)	(2)	(3)	(4)	(5)	(6)	(7)	(8)	(9)	(10)	(11)
Streamline deck, $V_u = 0.41\,\text{cm/s}$, $h_u = 25\,\text{cm}$, $b = 3.78\,\text{cm}$										
22.0	3.00	1.21	0.404				0.120	1.25	2.76	Case 2
20.5	3.78	2.32	0.615				0.156	2.24	-3.59	Case 3
19.0	3.78	2.49	0.660				0.166	2.44	-1.90	Case 3
17.5	3.78	2.78	0.736				0.178	2.68	-3.46	Case 3
16.0	3.78	3.02	0.799				0.191	2.96	-1.99	Case 3
14.5	3.78	3.16	0.837				0.207	3.27	3.25	Case 3
13.0	3.78	3.63	0.960				0.225	3.61	-0.48	Case 3
11.5	3.78	3.88	1.028				0.247	3.98	2.47	Case 3
Deck with 6-girders, $V_u = 0.41\,\text{cm/s}$, $h_u = 25\,\text{cm}$, $b = 5.82\,\text{cm}$										
22.0	3.00	3.52	–				–	–	--	Case 1: NA
20.5	4.50	4.62	–				–	–	--	Case 1: NA
19.0	5.82	5.40	0.928				0.234	5.64	4.45	Case 2
17.5	5.82	6.00	1.032				0.250	6.02	0.33	Case 2
16.0	5.82	6.50	1.118				0.267	6.42	-1.29	Case 3
14.5	5.82	6.91	1.188				0.286	6.83	-1.16	Case 3
13.0	5.82	7.28	1.252				0.309	7.26	-0.25	Case 3
11.5	5.82	7.59	1.305				0.336	7.71	1.64	Case 3
Deck with 3-girders, $V_u = 0.41\,\text{cm/s}$, $h_u = 25\,\text{cm}$, $b = 7\,\text{cm}$										
22.0	3.00	4.68	–				–	–	--	Case 1: NA
20.5	4.50	5.97	–				–	–	--	Case 1: NA
19.0	6.00	6.88	–				–	–	--	Case 1: NA
17.5	7.06	7.59	1.075				0.288	7.67	1.06	Case 2
16.0	7.06	8.17	1.157				0.306	8.10	-0.84	Case 3
14.5	7.06	8.66	1.226				0.328	8.55	-1.27	Case 3
13.0	7.06	9.09	1.287				0.352	9.02	-0.80	Case 3
11.5	7.06	9.46	1.340				0.384	9.51	0.51	Case 3

Note: NA for Case 1 means "Not Applicable."